Antipodal Dual Exponentially Tapered Slot Antenna (DETSA) with Stepped Edge Corrugations for Front-to-back Ratio Improvement

Ting-Jui Huang and #Heng-Tung Hsu
Department of Communication Engineering, Yuan Ze University
135 Yuan-Tung Rd., ChungLi, Tao-Yuan 320, Taiwan, htbeckhsu@saturn.yzu.edu.tw

Abstract

We investigate the effect of stepped edge corrugations on the front-to-back ratio (F/B ratio) improvement for the antipodal DETSA. Three types of corrugation configurations with different combinations of slit length are investigated. The results revealed that the improvement in F/B ratio is directly related to the arrangement in corrugation configurations.

Keywords : DETSA Corrugation Front-to-back ratio

1. Introduction

Owing to the moderately high gain, wide operation bandwidth, symmetric radiation pattern in an endfire sense, and relatively low sidelobe level (SLL), Tapered slot antennas (TSA) have been very popular in ultra-wideband applications such as ground penetration, through-wall imaging, security, surveillance, and medical imaging [1,2]. With the first introduction of the "Vilvaldi" antenna by Gibson in 1979, thorough investigation of similar antenna types including linearly tapered (LTSA) and constant width (CWSA) have been reported in [3]. To date, various geometric profiles for the taper have also been developed [4-7].

Different from the Vivaldi antenna structure, the additional outer taper of the DETSA provides more degree of freedoms for design. Very detailed analysis on the geometrical dependence of the antenna characteristics have been reported in [8-9]. In terms of practical system level implementation, it is always desired that the antenna should have as high F/B ratio as possible. Edge corrugations have been proven successful in tapered slot antenna structures for F/B ratio improvement [6, 7]. However, current configuration of edge corrugations cannot effectively provide the improvement over a wide frequency band. In this paper, we proposed a new stepped corrugation structure to improve the F/B ratio for the DETSA with antipodal feeding structure. Three types of corrugation configurations with different combinations of slit length are investigated.

2. Benchmark Antenna Design

Fig.1(a) shows the geometry of the dual exponentially tapered slot antenna (DETSA) designed for benchmark purpose. In this design, the antipodal feeding structure is also included. The exponential function $y = a\exp(bx^c)$ was used with a=0.07, b=0.06988, c=1; and a=1.17, b =3.53187, c =6 to generate the inner and outer taper profiles respectively. All the other geometrical parameters involved are W=78.76mm, W_o=36.26mm, W_f=1.1mm, L=91mm, and L_2=16mm. The length of the antenna was kept at about one wavelength in freespace at the center frequency. CST Studio Suite 2010 was adopted as the main simulator [10]. The design was implemented on RO4003 with dielectric constant of 3.38 and thickness of 0.508mm. Fig.2 shows the measured S_{11} and gain of the prototype with simulation results included for comparison. Fig. 3 shows the corresponding radiation patterns on E- and H-plane at 6GHz. The correctness of the simulation results was validated by the measurement.

3. Effect of Conventional Edge Corrugation on F/B Ratio

Investigation of the effect on the F/B ratio due to conventional edge corrugation was firstly performed through numerical simulation. Fig. 1(b) shows the structure of interest where the conventional configuration for edge corrugation is applied to the benchmark design. At fixed S_w=1mm, the F/B ratio compared to that of the benchmark antenna for the cases of three different depths *sl*, corresponding to quarter wavelength at 4GHz, 6GHz and 8GHz were plotted in Fig. 4. Apparently, edge corrugation does improve the F/B ratio at certain range of frequencies. Interestingly, one may observe that the F/B ratio is actually worse than the benchmark antenna even with corrugation for 8GHz, 12GHz, and 16GHz at which *sl* corresponds to half wavelength. Such deterioration in F/B ratio can well be explained through the current distribution shown in Fig. 5.

4. The Stepped Corrugation Configuration

Fig. 1(c) shows the proposed structure with the stepped corrugation configuration. Instead of a single slit as the conventional configuration, a stepped configuration is proposed here. Since the width of the slits will not have much effect as discussed in [6,7], such arrangement of different length *sl1* and *sl2* in each slit can be interpreted as the combination of slits corresponding to two different frequencies. In the discussions here, we investigate three types of combinations. For Type I, the *sl1* and *sl2* were chosen to be quarter wavelength at 4GHz and 6GHz. For Type II, the *sl1* and *sl2* were chosen to be quarter wavelength at 4GHz and 8GHz. For Type III, the *sl1* and *sl2* were chosen to be quarter wavelength at 6GHz and 8GHz.

Fig. 6 shows the measured S_{11} of Type I antenna with simulated results included. The farfield radiation patterns of the same antenna are shown Fig. 7. The effect of F/B ratio improvement due to stepped corrugation is clearly observed. Fig.8 shows the measured F/B ratio of the three types with that of the benchmark included. We can conclude that Type III antenna has the best performance in providing F/B ratio improvement in a broadband sense. The overall antenna characteristics of the three types together with the benchmark are listed in Table1.

5. Summary

In this paper, the effect of stepped edge corrugation on the F/B ratio for antipodal dual exponentially tapered slot antennas has been carefully investigated. Three different types corresponding to different combination in frequencies were compared against the benchmark design. From the experimental results, Type III antenna exhibited the best performance among the three types since an F/B ratio improvement in a broadband sense was achieved.

References

[1] C. T. Rodenbeck, S.-G. Kim, W.-H. Tu, M. R. Coutant, S. Hong, M. Li, and K. Chang, "Ultra-wideband low-cost phased-array radars," *IEEE Trans. Microwave Theory and Tech.*, vol. 53, n0.12, pp.3697-3703, Dec. 2005.

[2] "Ultra-wideband transmission systems, first report and order," FCC, Washington, DC, FCC 02-48, Apr. 2002.

[3] K. S. Yngvesson, D. H. Schaubert, T. L. Korzeniowski, E. L. Kolberg, T. Thungren and J. F. Johansson, "Endfire tapered slot antennas on dielectric substrate," *IEEE Trans. Antennas Propag.*, vol. AP-33, no.12, pp. 1392-1400, Dec. 1985.

[4] D.-C. Chang, B.-H. Zeng and J.-C. Liu, "Modified antipodal Fermi antenna with piecewise-linear approximation and shaped-comb corrugation for ranging applications," *IET Microw., Antennas Propag.*, vol. 4, Iss. 3, pp. 399-407, 2010.

[5] N. Symeon, G. E. Ponchak, J. Papapolymerou, and M. M. Tentzeris, "Conformal double exponentially tapered slot antenna (DETSA) on LCP for UWB applications," *IEEE Trans. Antennas Propag.*, vol. 54 , no.6, pp. 1663-1669, 2006.

[6] S. Sugawara, Y. Maita, K. Adachi, and K. Mizuno, "A mm-wave tapered slot antenna with improved radiation pattern," *IEEE MTT-S IMS Dig.* pp. 959-962, 1997.
[7] S. Sugawara, Y. Maita, K. Adachi, and K. Mizuno, "Characteristics of a mm-wave tapered slot antenna wit corrugated edges," *IEEE MTT-S IMS Dig.* pp. 533-536, 1998.
[8] Marc C. Greenberg and Kathleen L. Virga, "Characterization and design methodology for the dual exponentially tapered slot antenna," 1999 *IEEE Antennas and Propagation Society International Symposium*, pp.88-91.
[9] Marc C. Greenberg, Kathleen L. Virga, and Cynthia L. Hammond, "Performance characteristics of the dual exponentially tapered slot antenna (DETSA) for wireless communications applications," IEEE Trans. On Vehicular Technology, Vol. 52, No.2, pp.305-312, March 2003.
[10] CST Studio Suite 2010, www.cst.com

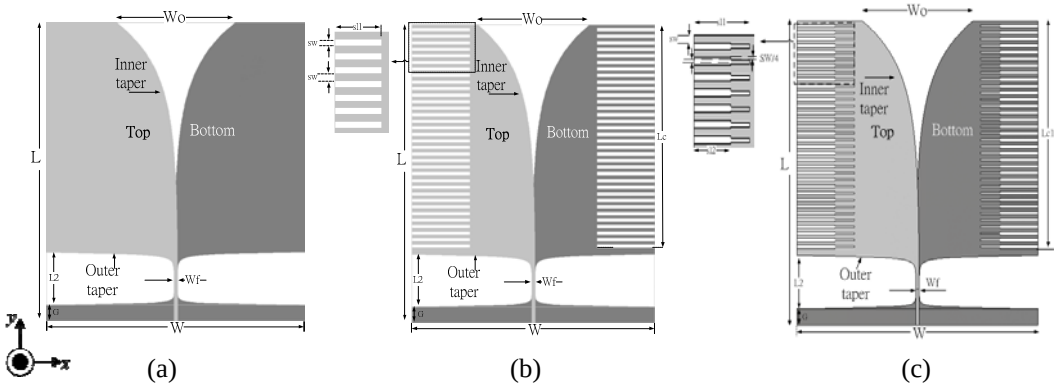

Fig.1 Geometries of the antipodal DETSA: (a) benchmark design without corrugation, (b) with conventional edge corrugation and (c) the proposed stepped corrugation structure.

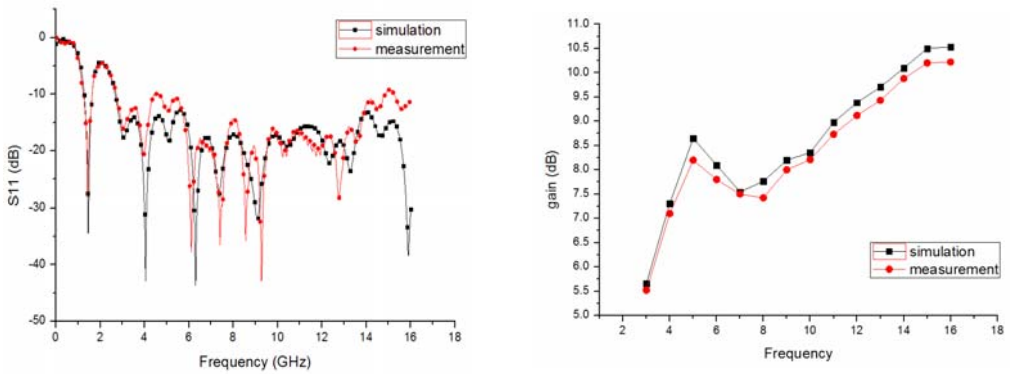

Fig.2 Measured and simulated S_{11} and gain of the benchmark antenna

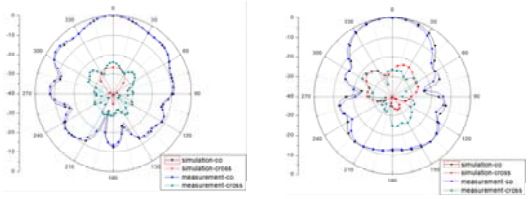

Fig.3 Measured and simulated patterns for E- (left) and H-plane (right) at 6GHz.

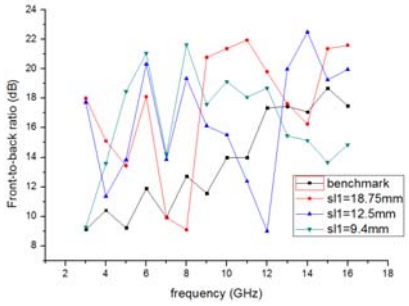

Fig. 4 Comparisons of F/B ratio for the cases of different corrugation depth

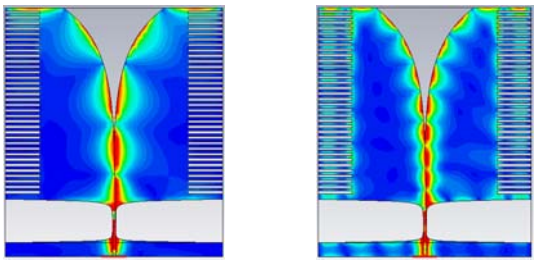

Fig.5 Current distributions for sl1=12.5mm at 6GHz (left) and 12 GHz (right)

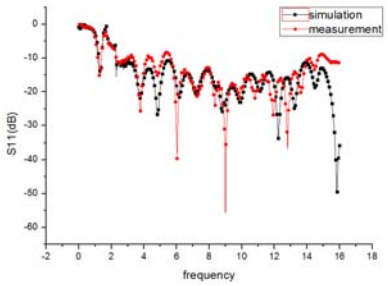

Fig. 6 Measured and simulated S11 of Type I antenna

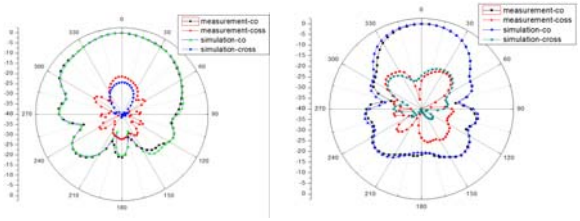

Fig.7 Measured and simulated patterns for E- (left) and H-plane (right) of Type I ant at 6GHz.

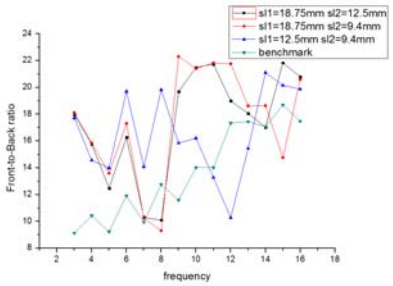

Fig. 8 Comparisons of F/B ratio for the three types of antennas

Table 1. Summary of Antenna Characteristics for Three Antennas

	Freq	3dB beam-width E-plane/H-plane (deg)	F/B Ratio E-plane (dB)	Peak Gain E-plane (dB)
Benchmark	3GHz	82.9 / 127.9	9.15	5.58
	7GHz	87.5 / 57.2	11.48	7.4
	11GHz	53.7 / 56.9	15.35	8.74
Type I	3GHz	60.6 / 121.3	20.2	7.4
	7GHz	92.5 / 54.5	11.089	7.05
	11GHz	49.2 / 62.4	20.87	9.07
Type II	3GHz	60.3 / 120.6	21	7.53
	7GHz	93.1 / 54.5	11.1	7
	11GHz	49.1 / 62.1	20.36	9.05
Type III	3GHz	47.9 / 109.0	21.17	8.67
	7GHz	94.8 / 55.9	15.84	6.9
	11GHz	57.5 / 59.1	13.77	8.7